

## Supplementary Information

### **Quantitative analysis of the effects of vimentin intermediate filaments on the early stages of influenza A virus infection**

Ju-Mei Zhang<sup>#a</sup>, Zhi-Gang Wang<sup>#b</sup>, Lei Du<sup>a</sup>, Dan-Dan Fu<sup>a</sup>, Meng-Qian Zhang<sup>b</sup>, Jing Li<sup>a</sup>, Shu-Lin Liu<sup>b</sup>, Dai-Wen Pang<sup>\*ab</sup>

<sup>a</sup>College of Chemistry and Molecular Sciences, Wuhan University, Wuhan 430072, P. R. China.

<sup>b</sup>State Key Laboratory of Medicinal Chemical Biology, Tianjin Key Laboratory of Biosensing and Molecular Recognition, Research Center for Analytical Sciences, College of Chemistry, and School of Medicine, Nankai University, Tianjin 300071, P. R. China.

\*E-mail: [dwpang@whu.edu.cn](mailto:dwpang@whu.edu.cn).

#### Contents

1. Viability of MDCK cells under different treatments.
2. Evaluation of labeling efficiency of QD705 labeling IAV envelope.
3. Visualization of the infection of QD705-H9N2 virus in Vim-KD MDCK cells.
4. Definition of cell boundary.
5. Typical trajectory of QD705-H9N2 virus and the time it went through rapid movement.
6. Visualizing the infection of QD705-H9N2 virus in MDCK cells transfected with EGFP-Vimentin and tdTommatto-MAP4.
7. Visualizing QD705-H9N2 virus infecting MDCK cells transfected with EGFP-Vimentin and mCherry-Rab7a.
8. Colocalization of QD705-H9N2 virus with Rab7 after rapid movement.
9. Acidic endosomes stained with LysoSensor Green DND-189.
10. Optimization of the concentration of cycloheximide.
11. Table 1. Summary of four types related to endosome during IAV infection.
12. Legends for Movie S1-S4.

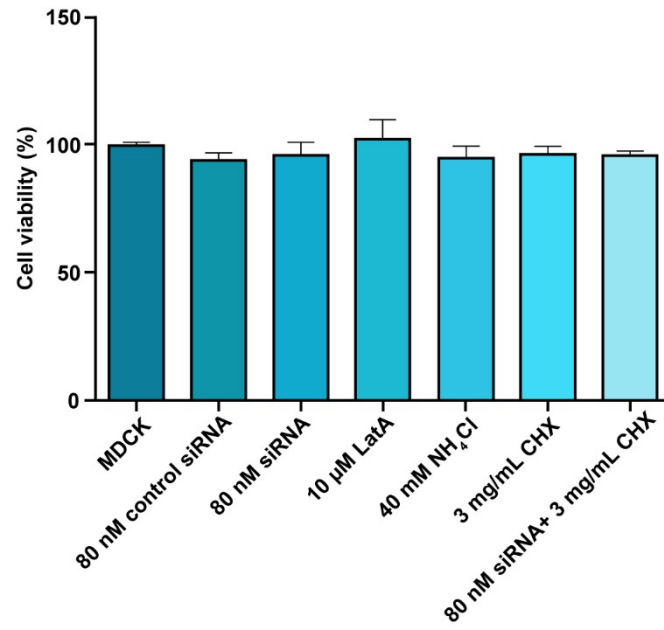


**Figure S1.** Viability of MDCK cells under different treatments. After siRNA transfected for 72 h or MDCK cells cultured for 72 h, different inhibitors were added and incubated for another 2 h.

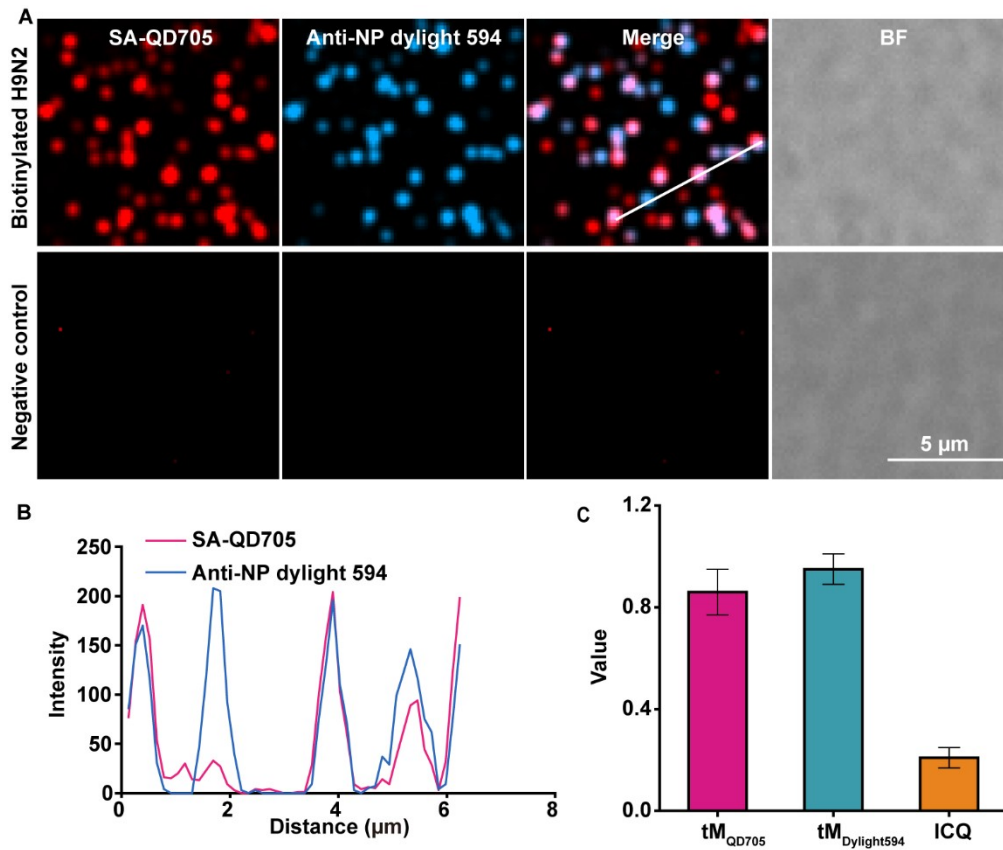


**Figure S2.** Evaluation of labeling efficiency of QD705 labeling IAV envelope. (A) Immunofluorescence images of biotinylated H9N2 (above) and PBS buffer (below) labeled by QD705 (red) and anti-NP antibody (blue) absorbed on the bottom of glass-bottom culture dishes. (B) Line profile showing distributions of the signals on the line in A. (C) The  $tM_{QD705}$  ( $86.0 \pm 9.0\%$ ),  $tM_{DyLight594}$  ( $95.0 \pm 6.0\%$ ) and ICQ ( $0.209 \pm 0.04$ ) values calculated from 5 random regions, an average of 107 particles were calculated for each region. The  $tM_{QD705}$  ( $tM_{DyLight594}$ ) means the percentage of QD705 (NP-dyLight594) signals colocalized with NP-dyLight594 (QD705) signals in the corresponding threshold image. ICQ is an intensity correlation quotient, and its value between 0.1 and 0.5 indicates that the two signals are strongly correlated.

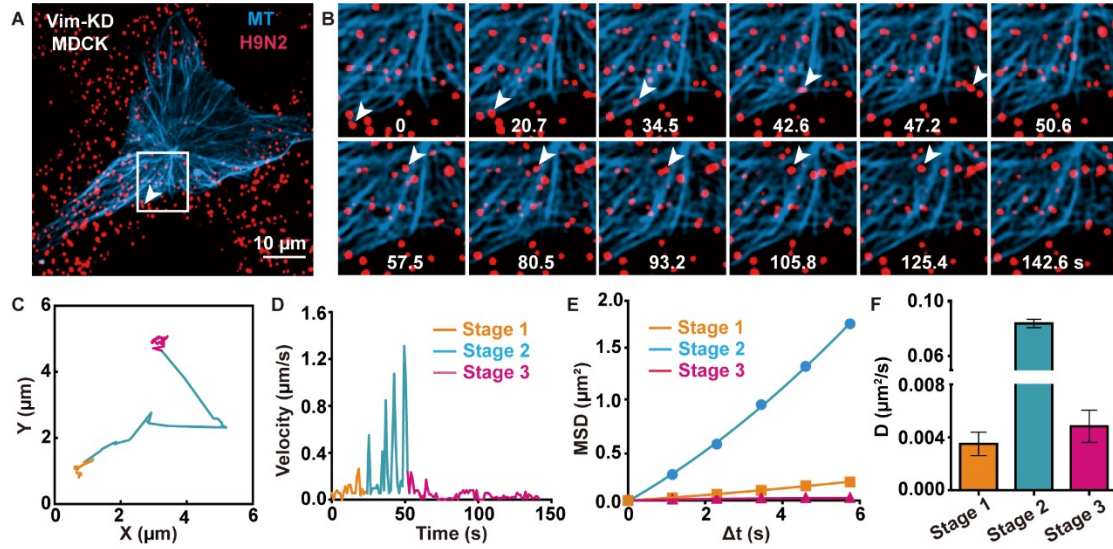


**Figure S3.** Visualization of the infection of QD705-H9N2 virus in Vim-KD MDCK cells. (A) Fluorescence image of QD-H9N2 (red) infected in Vim-KD MDCK cells transfected with GFP-MAP4 (blue). (B) Montage of the time series of the QD705-H9N2 (red) moving along the MT (blue) in the region of interest (ROI) in A. (C, D) Typical trajectory and time trajectory of the instantaneous velocity of QD-H9N2 shown in (B). (E) MSD-time plots in stage 1-stage 3 (orange, blue and pink, respectively), and the lines are fit to  $MSD = 4D\Delta t + (V\Delta t)^2 + \text{constant}$ . (F) Diffusion coefficient (D) statistics of the three stages, in which the average D are  $0.0035 \pm 0.00089 \mu\text{m}^2/\text{s}$  (stage 1),  $0.083 \pm 0.0029 \mu\text{m}^2/\text{s}$  (stage 2) and  $0.0048 \pm 0.0012 \mu\text{m}^2/\text{s}$  (stage 3).

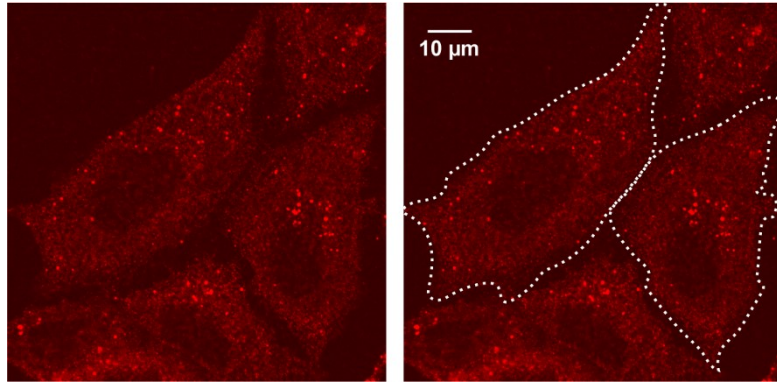


**Figure S4.** Definition of cell boundary. Raw image of SA-Cy3 labeled internalized IAV (red) after removing the biotin on the surface of the uninternalized virus by MESNA (left). An outline drawn according to the nonspecific adsorption signals of SA-Cy3 in the whole cell (right).

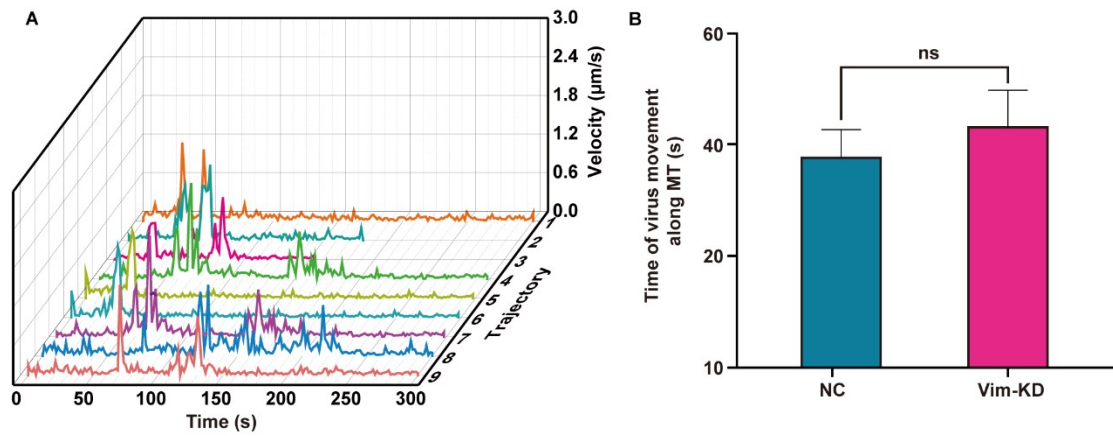


**Figure S5.** (A) Nine typical trajectories of QD705-H9N2 viruses extracted from Vim-KD MDCK cells. The viruses still moved with the three-stage of “slow-fast-slow” mode. (B) Statistics of the time of virus moving along microtubule (MT); ns  $P > 0.05$ .

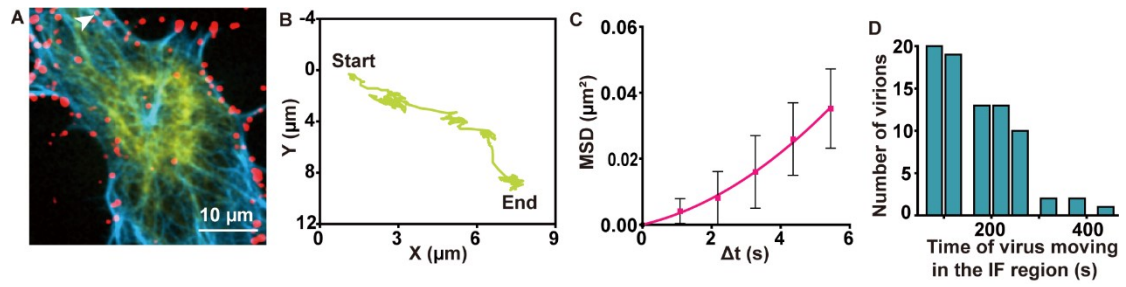


**Figure S6.** Visualizing the infection of QD705-H9N2 virus (red) in MDCK cells transfected with EGFP-vimentin (yellow) and tdTommatto-MAP4 (blue). (A) Image of vimentin IFs (yellow), microtubule (blue) and QD705-H9N2 (red). (B) The typical trajectory of QD705-H9N2 virus shown by the white arrow in A. (C) MSD fitting curve of QD705-H9N2 virus movement in vimentin IFs-dense area around MTOC. The line was fit to  $MSD = 4D\Delta t + (V\Delta t)^2 + \text{constant}$ . (D) Histogram of time distribution of QD705-H9N2 viruses in vimentin IFs-dense area.

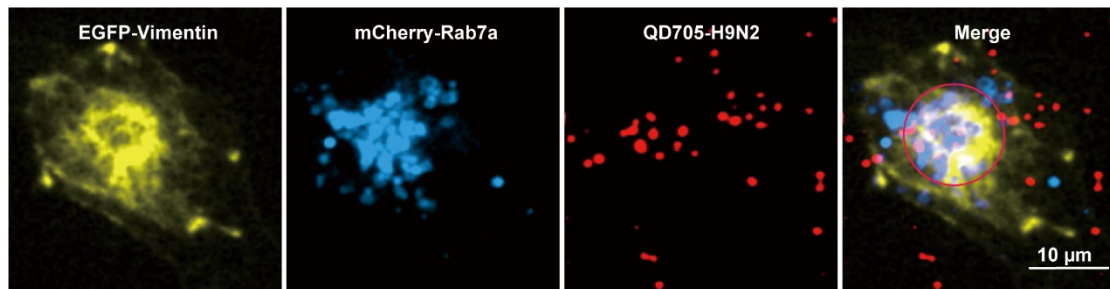


**Figure S7.** Visualizing QD705-H9N2 virus (red) infecting MDCK cells transfected with EGFP-Vimentin (yellow) and mCherry-Rab7a (blue). The red circle shows that most QD705-H9N2 viruses can colocalize with Rab7 in the vimentin IFs-dense area.

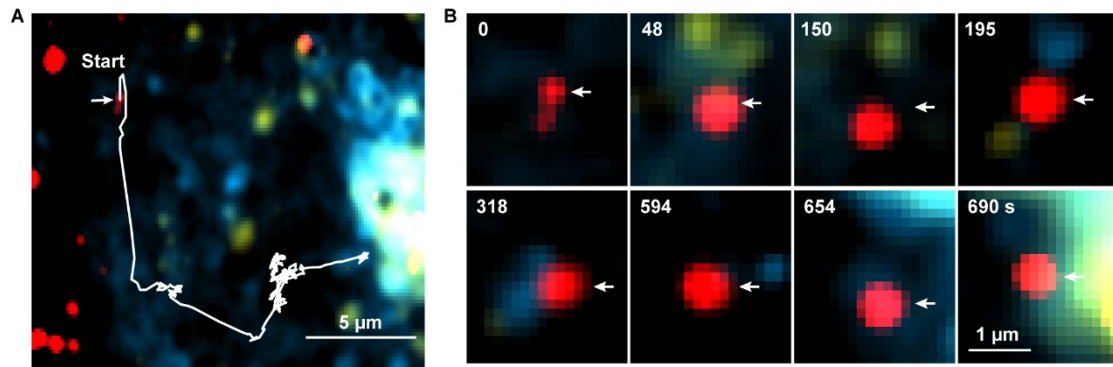


**Figure S8.** Colocalization of QD705-H9N2 virus with Rab7 after rapid movement. (A) Fluorescence image of ROI when QD705-H9N2 virus (red) infecting MDCK cell transfected with EGFP-Rab5a (yellow) and mCherry-Rab7a (blue) and their typical trajectories (white line). (B) Montage of the time series of the relationship between the QD705-H9N2 virus (white arrow in A) and endosomes.

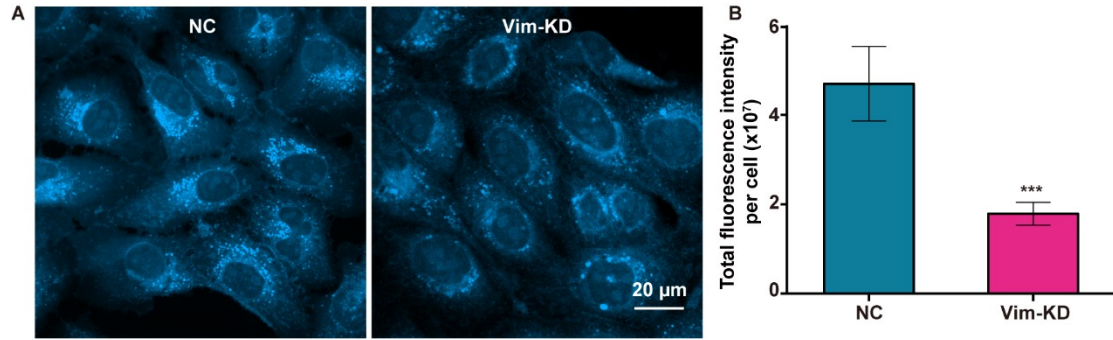


**Figure S9.** (A) Acidic endosomes in control and Vim-KD MDCK cells stained with LysoSensor Green DND-189 (blue). (B) Fluorescence intensity statistics in cells (100 cells of each group were counted); \*\*\* $P < 0.001$ .

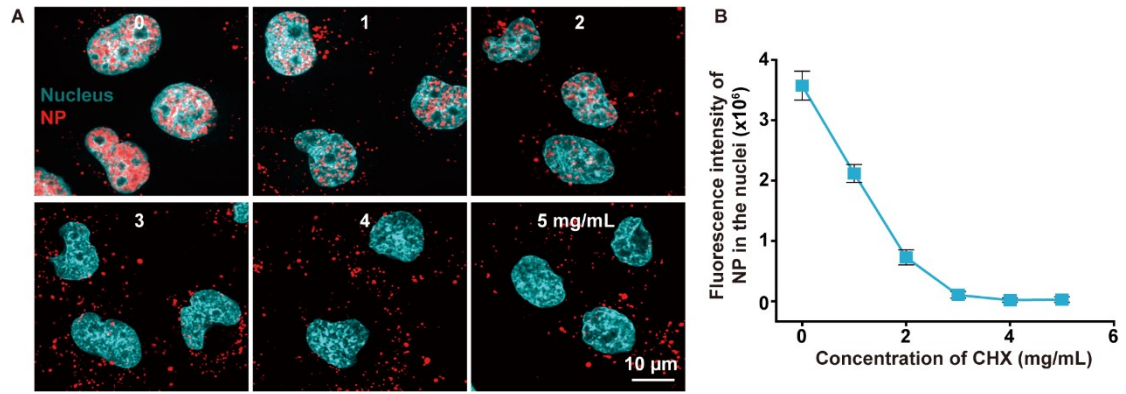


**Figure S10.** Optimization of the concentration of cycloheximide. (A) Immunofluorescence images of IAV (MOI=10) infecting MDCK cells treated with different concentrations of cycloheximide for 1 hour and using dylight488 labeled anti-NP antibody (red) and Hoechst33342 (cyan) to stain cells. (B) Statistical analysis of fluorescence intensity of NP signal in the nuclei (30 cells were counted at each concentration).

**Table 1.** Summary of four types related to endosomes during IAV infection.

type	Detail	Proportion (%)	
		Control cell	Vim-KD cell
Always in EE	IAV colocalizes with Rab5 during fast movement until the end.	9.0	34.6
Finally in ME	After colocalizing with Rab5 and experiencing fast movement, IAV colocalizes with Rab5 and Rab7 in the perinuclear area with a slow movement	56.5	50.3
Finally in LE	After colocalizing with Rab5 and experiencing fast movement, IAV colocalizes with Rab5 and Rab7 and finally colocalizes with Rab7 in the perinuclear area with a slow movement	24.5	7.5
	In the fast movement stage, it has nothing to do with Rab5, but colocalizes with Rab7 in the perinuclear area and moves slowly.	5.0	1.3
Neither in EE nor in LE	During the imaging time, the process of virus infection with obvious long-distance movement had nothing to do with Rab5 and Rab7.	5.0	6.3

**Movie S1.** QD705-H9N2 virus (red) experienced rapid movement in the early endosome (yellow) to reach the perinuclear region and remained in the early endosome.

**Movie S2.** After rapid movement, QD705-H9N2 virus (red) finally colocalized with Rab5 (yellow) and Rab7 (blue) (maturing endosome) in the perinuclear region.

**Movie S3.** After the rapid movement of QD705-H9N2 virus (red), it finally enters the late endosome (blue). (A) After rapid movement, QD705-H9N2 virus (red) colocalizes with Rab5 (yellow), Rab7 (blue) in the perinuclear region, and finally with Rab7. (B) After rapid movement, QD705-H9N2 virus (red) colocalizes directly with Rab7 in the perinuclear region.

**Movie S4.** The QD705-H9N2 virus (red) experiences rapid movement but has nothing to do with Rab5 (yellow) and Rab7 (blue).